Feasibility of Passive Electromagnetic Dampers as Energy Harvesters in Large Structures

by

Christopher Hendrix

Bachelor of Science in Civil and Environmental Engineering
Massachusetts Institute of Technology, 2012

SUBMITTED TO THE DEPARTMENT OF CIVIL AND ENVIRONMENTAL ENGINEERING IN PARTIAL FULFILLMENT OF THE REQUIREMENTS FOR THE DEGREE OF

MASTER OF ENGINEERING IN CIVIL AND ENVIRONMENTAL ENGINEERING

AT THE

MASSACHUSETTS INSTITUE OF TECHNOLOGY

June 2013

Signature of Author:_____
Department of Civil and Environmental Engineering
May 21, 2013

Certified by:_____
Jerome J. Connor
Professor of Civil and Environmental Engineering
Thesis Supervisor

Accepted by:_____
Heidi M. Nepf
Chair, Departmental Committee for Graduate Students

Feasibility of Passive Electromagnetic Dampers as Energy Harvesters in Large Structures

by

Christopher Hendrix

Submitted to the Department of Civil and Environmental Engineering on May 21, 2013 in partial fulfillment of the requirements for the Degree of Master of Engineering in Civil and Environmental Engineering at the Massachusetts Institute of Technology.

Abstract

There has been a trend in structural design toward energy efficient design and motion based design. The strategy of motion based design is controlling the movement of structures to meet certain dynamic response requirements by damping the structure. Structural damping dissipates the energy of external loads internally within the structure. A simple idea is to connect the two design strategies to control the motion of a structure while harvesting this dissipated energy by transducing it to electrical energy via passive electromagnetic damping. This study will attempt to determine the feasibility of using passive electromagnetic damping to control the motion and harvest the energy of damping of large scale structures.

Thesis Supervisor: Jerome J. Connor

Title: Professor of Civil and Environmental Engineering

Table of Contents

Figures

1 Introduction

In large scale structural design, two design processes in particular have been gaining importance. The first is the design of energy efficient structures. A structure that is efficient in its energy usage can be beneficial both economically by saving money on energy costs and environmentally by reducing the amount of carbon released into the atmosphere.

Another trending design process is motion based design. Motion based design is a design strategy that limits the response of a structure due to dynamic loading (i.e. earthquakes, wind, waves, etc.). A way to reduce the response of a structure is by dissipating the external, input energy within the structure of a building. Energy is dissipated internally in structures via damping. As buildings become more flexible, new technologies require a manufacturing process devoid of external movement, and the technology of new materials fail to develop an increase of material stiffness, there is an increase of importance of motion based design (Connor, 2003).

1.1 Motivation

The idea of combining both motion based design and energy efficient design is simple. If a strategy of motion based design is dissipating external energy internally, how can we harvest this energy? There are several dampers available that can create electrical energy via damping, with the main two being piezoelectric materials and electromagnetic (EM) dampers. It has been shown that piezoelectric materials and EM dampers are successful at harvesting energy on a small scale (i.e. car suspension). At a small scale, material costs of piezoelectric materials and EM dampers are much lower because the impact of the high cost of material and magnet technology is low. The motivation behind this research, however, is to determine the feasibility of harvesting electricity via EM damping for larger scale structures.

1.2 Scope

The scope of this research is to first understand the fundamental physics behind electromagnetic dampers and structural dynamics. A simple electromagnetic model will be provided and a relationship between the force, velocity, and energy dissipated will be determined. The response of single degree of freedom (SDOF) and multiple degree of freedom (MDOF) systems will also be discussed.

Secondly, two models of a SDOF toy will be analyzed. The first model will attach a sample EM damper in parallel with the damper already installed on the toy. The second model has a mass attached to the toy with an EM damper that is tuned to be a tuned mass damper (TMD). The change of the control toy's response due to these damping strategies along with the energy each strategy creates will be compared.

Thirdly, a real world passive EM damper will be described and a sample large scale damper will be designed to be a tuned mass damper for the six-story structure analyzed in the last section of this research. Damper properties and the cost of the sample TMD EM damper will be given.

Finally, a sample six-story structure will be analyzed by attaching a mass to the top floor of the structure using the aforementioned damper. The EM damper and the mass attached to the damper will be tuned so that the system acts like a TMD for the first fundamental mode. The building will be undergo two sample loadings: 1) wind loading at each node developed from high resolution wind data, 2) earthquake loading developed from data of the El Centro earthquake. The reduction in motion due to the TMD for both cases will be plotted. The energy harvested in both loading cases will also be calculated. By comparing the cost of the dampers and the amount of energy saved by passive EM damping system, the feasibility of using EM dampers as energy harvesters will be discussed.

2 Literature Review

Harvesting energy through electromagnetic dampers is a well study topic in the mechanical, electrical, and civil engineering communities. Several small scale EM dampers have been modeled, designed, and successfully tested for vehicle suspension. However, the feasibility of damping large scale structures with EM dampers has still yet to be fully determined. This section will discuss several relevant studies to the topic of this paper.

2.1 EM Dampers for Large Structures

Palomera-Arias (2005) has done an in depth feasibility study of the use of passive electromagnetic dampers for the motion control of large structures, including an economic analysis. In the study, it is determined that a tubular coiled machine with a moving magnet is the most suitable of tubular designs, and a relationship between the linear velocity and the magnetic force of a specific tubular EM damper is developed. An example on how this specific damper can be optimized to for inner-story damping is given. Finally, experiments were performed with a tubular damper in order to compare the mathematical model with a real model. Experiment results were within 20% of the predicted results. Through this analysis, it was determined that tubular, passive electromagnetic dampers cost five times that of fluid dampers in order to achieve similar damping and therefore are not feasible until magnet technology is enhanced and magnet prices drop (magnets are the main factor in the price of an EM damper).

Tang and Zuo (2012) designed an electromagnetic TMD and corresponding circuits that will result in active, semi-active and passive damping. The energy storage mechanism of these circuits is a battery. The circuit designed for semi-active control includes an inductive electromagnetic motor and a switch that, when on, provides the maximum damping capacity of the EM motor and will turn off once the velocity of the motor dips below a certain magnitude. The circuit design for self-powered active control, is similar to that of the semi-active circuit with the addition of two switches. The duty cycles of the switches in the active circuit are able to control the driving force. The passive damping coefficient can be adjusted by changing the equivalent resistance of the passive EM circuit. Tang and Zuo built a small scale building (1.9 m tall) and tested each damping strategy using a small scale TMD. Results of the experiment show that the switch from active to semi-active to passive damping results in a decreasing ability to mitigate vibration and an increasing ability to harvest

energy. No comments are provided on the whether each damping strategy will harvest enough energy at a larger scale to be feasible.

2.2 EM Dampers for Smaller Scale Applications

Ebrahimi et al (2009) tested the feasibility of a passive electromagnetic damper for use in vehicle suspension. He develops a mathematical model to relate the magnetic force created and the velocity of the mover moving the permanent magnets of a scaled down EM damper. He then optimizes the damper's parameters such as the air gap inside the damper and the magnet thickness. A damper is then created according to these optimized values. After running tests on the damper, he concludes that although his damper was too expensive and heavy and decreases the appeal for vehicle suspension, the use of EM dampers in vehicles is still attractive because the damper is non-contact, high durability, and has a simple design. He mentions nothing on harvesting the energy, however.

Zuo & Zhang, (2013) performed a study to try to determine the potential of harvesting power in vehicle suspension. A mathematical model of the damper was developed and sample parameters were given to the EM damper. The results of the model show that the absorbers have a 100-400 W average power dissipation potential for a mid-sized vehicle traveling at 60 mph. Zuo & Zhang estimate that energy could cause up to a 2-10% fuel efficiency increase, which is a relatively significant increase.

3 Electromagnetic Damping Theory

Electromagnetic dampers can be active, semi-active or passive. Active dampers in general take data from sensors that read external loading on a structure and the controller interprets this data and controls the properties of the damper so that the structure has the desired response (Connor, 2003). Electromagnetic dampers are good active dampers because the damping coefficient can be controlled by the amount of current and resistance in the circuit, which can adjust based on the controller output due to the sensor readings. Active dampers are useful because they can deliver a large force output in a short period of time (Connor, 2003). However, active dampers are not useful when trying to harvest energy because they require energy input.

Semi-active dampers turn on only when a force is needed. In the case of the electromagnetic damper, the force is opposite to the velocity of the mover. If the force required by the damper is in the same direction of the velocity, the force demand cannot be met. Therefore the actuator needs to be switched off until the phase changes direction (Connor, 2003).

A passive damper requires no input energy to function. The main function of a passive damper is to resist the movement of a particular structure by dissipating the energy of the structure. Passive dampers include viscous dampers, friction dampers, and rubber bearings. Damping is also lost in building frames inherently due to material deformation and connection slipping. The purpose of an energy harvesting electromagnetic damper is to transduce the mechanical energy dissipated of the structure to usable electrical energy while controlling the motion of the structure. The goal of this section is to understand the physics behind a passive, energy harvesting electromagnetic damper.

3.1 Simple Passive Model

Consider a sliding rod on conducting rails in a constant magnetic field connected to a circuit with a resistor, $R = R_{load}$, which supplies power to an external source . It can be assumed that the magnetic field is created by a ferromagnetic material (permanent magnet). To simplify the system, consider the model under theoretical conditions and assume there is no friction acting on the rails.

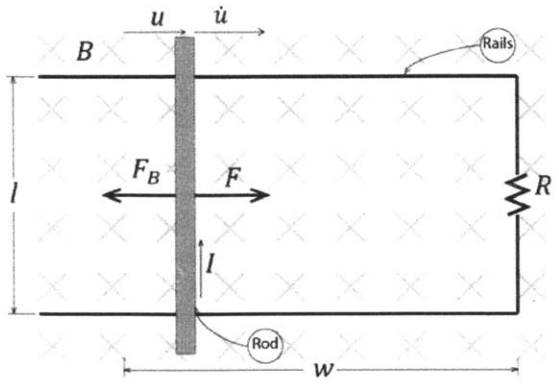

Figure 1. Sliding rod on rails.

3.2 Velocity and Force Relationship

Using electricity and magnetism concepts, a relationship between force an velocity can be determined for the model shown in Figure 1. The magnetic force on the rod of length $\vec{l}$ with a current I in a magnetic field $\vec{B}$ is:

$$\vec{F}_B = I\vec{l} \times \vec{B} \tag{1}$$

The magnetic flux through a given area, $\vec{A}$, that is perpendicular to the direction of the magnetic field is equal to the product of the area and the magnitude of the magnetic field. The flux in this model is time dependent on the displacement of the bar, u.

$$\Phi_B = \vec{B} \cdot \vec{A} = Bl(w + u(t)) \tag{2}$$

Faraday's law states that the induced emf, ε, is proportional to the change of flux over time. The change in flux with respect to time is determined by taking the derivative of Equation (2), where $\dot{u}$ is the velocity of the bar.

$$\varepsilon(t) = -\frac{d\Phi_B}{dt} = -Bl\frac{d}{dt}\big(w + u(t)\big) = -Bl\dot{u}(t) \tag{3}$$

If the machine constant is $K_t = -Bl$, the emf is equal to the product of the machine constant and the time varying velocity of the system and the magnetic force is equal to the machine constant times the time varying current.

$$\varepsilon(t) = K_t\dot{u}(t) \qquad F_B(t) = K_t I(t) \tag{4}$$

In the circuit in Figure 1, the voltage drop across the resistor must equal the induced emf:

$$\varepsilon - IR = 0 \tag{5}$$

Equation (5) can be modified using the relationships in Equation (4) to represent the equilibrium of electric potential:

$$K_t\dot{u} - \frac{F_B}{K_t}R = 0 \tag{6}$$

The magnetic force with respect to time in the circuit can be derived from Equation (6):

$$F_B(t) = \frac{K_t^2}{R}\dot{u}(t) \tag{7}$$

For this particular electromagnetic damper with the magnetic field flowing into the page, the current flows clockwise when the rod moves to the right and counter clockwise when the rod moves to the left. The direction of the magnetic force always opposes the direction of the velocity of the moving bar.

3.3 Energy Dissipation

Because there is always a force opposing the direction of the velocity in the system, there will be mechanical energy dissipation. If we consider Figure 1 an ideal model, the mechanical energy dissipated from the system will be in the form of electric energy dissipated over the resistor.

$$P_R = I^2R \tag{8}$$

Therefore the energy created by the system is the integral of the power dissipated by the resistor over a certain time interval:

$$W_R = \int_C P_R dt = \int_{t=0}^{t=T} I^2 R dt \tag{9}$$

4 Structural Dynamics

Large scale structures are designed for both static and dynamic loading. The damping of a is related to the dynamic movement of a structure. The motion of a structure caused by external dynamic loading and inertia forces can be modeled depending on the external load and the mass, stiffness, and damping properties of the structure. The material in this section will describe the response of both a single degree of freedom and a multiple degree of freedom system due to harmonic loading, harmonic support acceleration, and free vibration.

4.1 Single Degree of Freedom System

4.1.1 Equation of Motion

The movement of a single degree of system (Figure 2) subjected to a time varying force, $p(t)$, with a stiffness k, and a damping coefficient, c, can be modeled with the following equation of forces:

$$m\ddot{u} + c\dot{u} + ku = p(t) \tag{10}$$

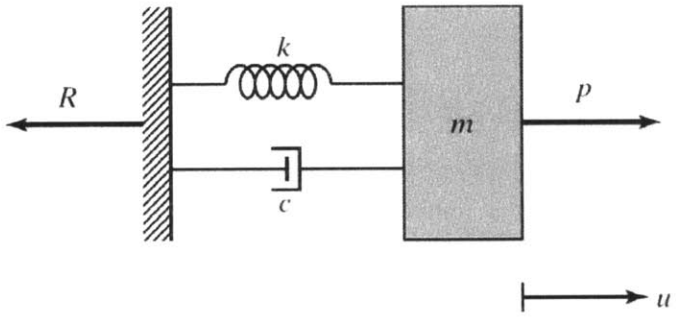

Figure 2. Single degree of freedom system

The natural frequency of the system can be described as the square root of the stiffness divided by the mass.

$$\omega_n = \sqrt{\frac{k}{m}} \tag{11}$$

The damping coefficient for a single degree of freedom system is shown in Equation (12) where ξ is the percent damping of the system (Connor, 2003).

$$c = 2\xi\sqrt{km} \tag{12}$$

The damped frequency of the system is the natural frequency scaled by the square root of one minus the percent damping (Kausel, 2009).

$$\omega_d = \omega_n\sqrt{1-\xi} \tag{13}$$

The properties of the structure described in Equations (11), (12), and (13) are important in determining the response of the system.

4.1.2 Response

The dynamic response of the single degree of freedom is the movement of the structure with respect to time. The homogeneous solution of the response with initial values of displacement, u_0, and velocity, $\dot{u}_0$, is as follows (Kausel, 2009):

$$u_h(t) = e^{-\xi\omega_n t}\left[u_0\cos(\omega_d t) + \frac{\dot{u}_0 + \xi\omega_n u_0}{\omega_d}\sin(\omega_d t)\right] \tag{14}$$

The particular solution can be calculated as the convolution integral between the time varying load, $p(t)$, and the impulse response function, $h(t)$.

$$u_p(t) = \int_0^t h(\tau)p(t-\tau)d\tau = h * p \tag{15}$$

where

$$h(t) = \frac{1}{m\omega_d}e^{-\xi\omega_n t} \tag{16}$$

The time varying displacement, $u(t)$, of the system with respect to the ground is the sum of the homogeneous solution and the particular solution:

$$u(t) = u_h(t) + u_p(t) \tag{17}$$

The responses due to a perturbation of the system are described in Table 1. For the response due to ground motion, the response is given in relative displacement, $v(t)$. For harmonic excitations, the tuning ratio can be defined as the forcing frequency divided by the natural frequency, $\rho = \Omega/\omega_n$.

Table 1. Responses of a SDOF system.

Perturbation Type	Loading	Response
a) Free vibration with an initial displacement u_0	$p(t) = 0$	$u(t) = u_0 \cos(\omega_d t) + \frac{\xi \omega_n u_0}{\omega_d} \sin(\omega_d t)$
b) Harmonic excitation with magnitude $\hat{p}$ and frequency Ω with no initial values	$p(t) = \hat{p}e^{\Omega t}$	$u(t) = h * (\hat{p}e^{\Omega t})$
c) Ground motion with magnitude with time varying acceleration $\ddot{u}_g$ and no initial values	$p(t) = -m\ddot{u}_g$	$v(t) = h * (-m\ddot{u}_g)$

4.2 Multiple Degree of Freedom Response

4.2.1 Equation of Motion

A depiction of a system with n degrees of freedom is shown in Figure 3. This model is displaced in lumped mass model form.

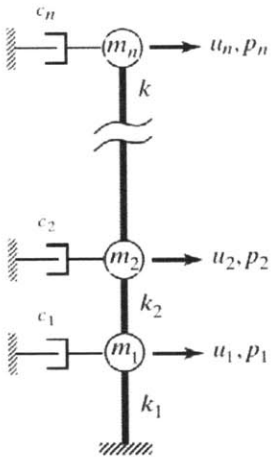

Figure 3. Lumped mass model depiction of a system with n degrees of freedom.

The mass matrix, stiffness matrix and the damping matrix can be developed as follows (Connor, 2003):

$$\mathbf{M} = \begin{bmatrix} m_1 & & 0 \\ & \ddots & \\ 0 & & m_n \end{bmatrix}$$

$$\mathbf{K} = \begin{bmatrix} k_1 + k_2 & -k_2 & 0 & \cdots & 0 & 0 & 0 \\ -k_2 & k_2 + k_3 & -k_3 & \cdots & 0 & 0 & 0 \\ & \ddots & \ddots & \ddots & & & \\ \vdots & & -k_i & k_i + k_{i+1} & -k_{i+1} & & \vdots \\ & & & \ddots & \ddots & \ddots & \\ 0 & 0 & 0 & \cdots & -k_{n-1} & k_{n-1} + k_n & -k_n \\ 0 & 0 & 0 & \cdots & 0 & -k_n & k_n \end{bmatrix}$$

$$\mathbf{C} = \begin{bmatrix} c_1 + c_2 & -c_2 & 0 & \cdots & 0 & 0 & 0 \\ -c_2 & c_2 + c_3 & -c_3 & \cdots & 0 & 0 & 0 \\ & \ddots & \ddots & \ddots & & & \\ \vdots & & -c_i & c_i + c_{i+1} & -c_{i+1} & & \vdots \\ & & & \ddots & \ddots & \ddots & \\ 0 & 0 & 0 & \cdots & -c_{n-1} & c_{n-1} + c_n & -c_n \\ 0 & 0 & 0 & \cdots & 0 & -c_n & c_n \end{bmatrix}$$

The loading and displacement vectors take the following form:

$$\mathbf{P} = \begin{bmatrix} p_1 \\ p_2 \\ \cdot \\ \cdot \\ \cdot \\ p_n \end{bmatrix} \qquad \mathbf{u} = \begin{bmatrix} u_1 \\ u_2 \\ \cdot \\ \cdot \\ \cdot \\ u_n \end{bmatrix}$$

The mode shape vector, $\boldsymbol{\Phi}$, of the MDOF system can be determined by using the following eigenvalue equation, where λ is a dimensionless eigenvalue:

$$(\mathbf{K} - \lambda\mathbf{M})\boldsymbol{\Phi} = \mathbf{0} \tag{18}$$

Each fundamental mode shape, $\boldsymbol{\phi_j} = [\phi_{j1}; \phi_{j2}; \ldots; \phi_{jn}]$, comprises the mode shape vector:

$$\boldsymbol{\Phi} = [\boldsymbol{\phi_1}, \boldsymbol{\phi_2}, \ldots \boldsymbol{\phi_j}] \tag{19}$$

Modal values can be determined for the system. Below are the modal mass, modal stiffness, and modal damping values for mode j.

$$\tilde{m}_j = \boldsymbol{\phi}_\mathbf{j}^\mathrm{T}\mathbf{M}\boldsymbol{\phi}_\mathbf{j} \qquad \tilde{k}_j = \boldsymbol{\phi}_\mathbf{j}^\mathrm{T}\mathbf{K}\boldsymbol{\phi}_\mathbf{j} \qquad \tilde{c}_j = \boldsymbol{\phi}_\mathbf{j}^\mathrm{T}\mathbf{C}\boldsymbol{\phi}_\mathbf{j}$$

and

$$\tilde{p}_j = \boldsymbol{\phi}_\mathbf{j}^\mathrm{T}\mathbf{P}$$

The equation of motion can now be written in modal form where q is the displacement parameter that defines the response of a mode of the system (Connor, 2003).

$$\tilde{m}\ddot{q} + \tilde{c}\dot{q} + \tilde{k}q = \tilde{p} \tag{20}$$

The natural frequency, damping coefficient, and damping frequency can be found for a particular mode by substituting the modal mass, stiffness, and damping into the corresponding values in Equations (11), (12), and (13).

4.2.2 Response

The displacement parameter that defines the response of the system can be calculated as follows if there are no initial values (Kausel, 2009):

$$q(t) = \tilde{h} * \tilde{p} \tag{21}$$

The modal impulse response function is in similar form to Equation (16) however the mass, natural frequency and damped frequency must be replaced by their respective modal values:

$$\tilde{h}_j(t) = \frac{1}{\tilde{m}_j \omega_d} e^{-\tilde{\xi}\omega_{n,j}t} \tag{22}$$

Finally, the response vector can be calculated for mode j:

$$\mathbf{u}(t) = q(t)\boldsymbol{\phi}_\mathbf{j} \tag{23}$$

The responses due to perturbations of the system are described in Table 2, where Γ is the sum of the mode shape vector for mode j ($\Gamma = \sum_n m_n \phi_{jn}/\tilde{m}_j$). Again, the response due to support motion is in terms of motion relative to the movement of the ground, $\mathbf{v}(t)$.

Table 2. Responses of a SDOF system.

Perturbation Type	Modal Loading	Response for Mode j
a) Harmonic excitation with magnitude $\widehat{\mathbf{P}}$ and frequency Ω with no initial values	$\tilde{p}(t) = \boldsymbol{\phi}_\mathbf{j}^\mathrm{T}\widehat{\mathbf{P}}\mathrm{e}^{\Omega \mathrm{t}}$	$\mathbf{u}(t) = \left[\tilde{h}_j * \left(\boldsymbol{\phi}_\mathbf{j}^\mathrm{T}\widehat{\mathbf{P}}\mathrm{e}^{\Omega \mathrm{t}}\right)\right]\boldsymbol{\phi}_\mathbf{j}$
b) Support motion with magnitude with time varying acceleration $\ddot{u}_g$ and no initial values	$\tilde{p}(t) = -\Gamma\tilde{m}\ddot{u}_g$	$\mathbf{v}(t) = \left[\tilde{h}_j * \left(-\Gamma\tilde{m}\ddot{u}_g\right)\right]\boldsymbol{\phi}_\mathbf{j}$

5 Toy Response using EM Damping

In this section, a theoretical single degree of freedom toy will have its response motion reduced by damping strategies using the theoretical energy harvesting, passive, electromagnetic damper as described in Section 3 with sample parameters. The motion of the control mass will be reduced using two damping strategies: 1) by adding the EM damper in parallel with the primary damper, and 2) by adding a TMD using the EM damper. The same damper will be used for both damping strategies in order for comparison.

5.1 Control Toy

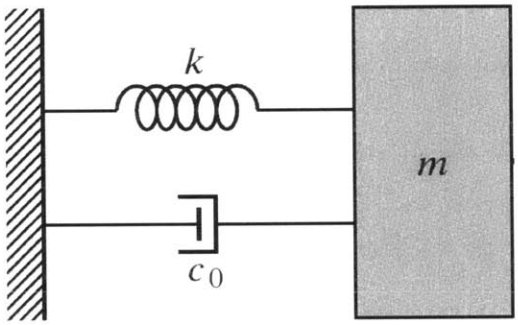

Figure 4. Control toy.

The control toy consists of a mass placed on a spring, k, and primary damper, c_0. A diagram of the model can be seen in Figure 4. The parameters of the model set up are described in Table 4.

Table 3. Model parameters.

Mass	m	1 kg
Stiffness	k	1 N/m
Primary damping	ξ_0	5%
Damping coeff	c_0	0.1 N-s/m
Natural frequency	ω_n	1.000 rad/sec

5.2 EM Damper

The damping force, F_d, is proportional to the product of a damping coefficient, c_d, and the time varying velocity of the system. If considering a freely vibrating system, the damping

force will slowly bring the moving system to rest. The higher the damping force, the quicker a freely vibrating system will come to rest.

$$F_d(t) = c_d\dot{u}(t) \tag{24}$$

For this single degree of freedom system, the EM damper circuit shown in Figure 1 will represent the electromagnetic damper in this model. By definition, it can be used as a damper because the force caused by the change of magnetic flux is proportional to velocity. Because of the relationship between Equations (7) and (24) , an equivalent damping coefficient, c_{eq}, can be determined. The equivalent damping for the model is as follows:

$$c_d = \frac{K_t^2}{R} \tag{25}$$

Using the relationship of Equations (12) and (25), an equivalent damping ratio can be determined.

$$\xi_d = \frac{K_t^2}{2R\sqrt{km}} \tag{26}$$

However, for the purpose of comparison between the TMD and the damper placed as an inner story damper, the resistance will be the resistance that corresponds to the optimal tuned mass damper damping ratio determined by Equation (28) ($\xi_d = \xi_{d,opt}$). Therefore the resistance is:

$$R = \frac{K_t^2}{2\xi_{d,opt}\sqrt{km}} \tag{27}$$

The table below shows the parameters of a sample damper. The resistance was calculated using Equation (27) and (28).

Table 4. Model damper parameters.

Resistance	R	34.26 Ω
Magnetic field	B	1.5 T
Moving rod length	l	50 cm

5.3 Inner Story Damped Toy

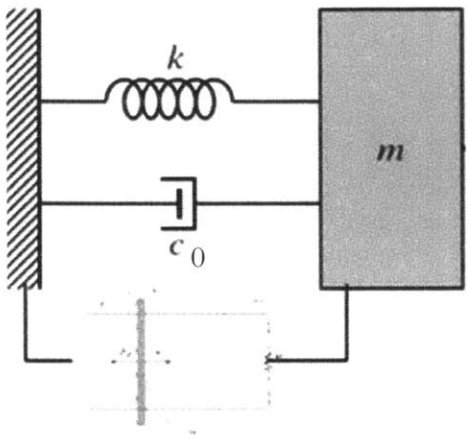

Figure 5. The inner story SDOF toy.

The toy that will represent a building with inner story damping will be a single degree of freedom model and the EM damper described in the previous section will be added in parallel with the initial damper ($c = c_d + c_0$) shown in Figure 4. Figure 5 depicts this.

5.4 Tuned Mass Damper Toy

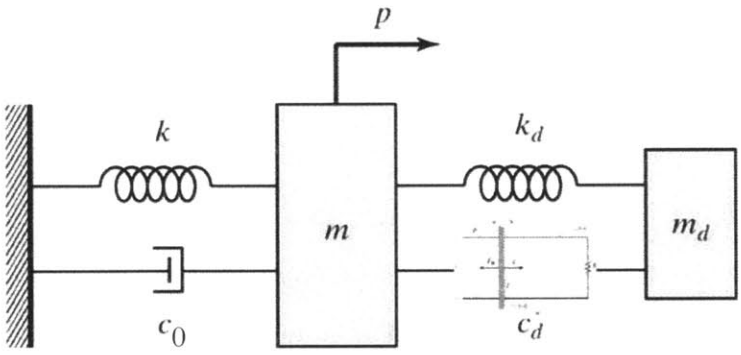

Figure 6. Tuned mass damper toy.

The tuned mass damper model will have a mass attached to the original SDOF system shown in Figure 4. The mass acting as the TMD will be 5% the weight of the original mass ($\bar{m} = 0.05$). Therefore, the optimal damping ratio can be determined.

$$\xi_{d,opt} = \sqrt{\frac{\bar{m}(3 - \sqrt{0.5\bar{m}}}{8(1+\bar{m})(1-0.5\bar{m})}} \tag{28}$$

The optimal natural frequency ratio can also be determined:

$$f_{opt} = \frac{\omega_d}{\omega} = \frac{\sqrt{1-0.5\bar{m}}}{1+\bar{m}} \tag{29}$$

Finally, the required stiffness of the attached mass can be calculated:

$$k_d = \bar{m} f_{opt}^2 k \tag{30}$$

The parameters for this particular model are shown in the following table.

Table 5. Parameters of the TMD model.

TMD mass	m_d	0.05 kg
TMD damping ratio	$\xi_{d,opt}$	0.1302
TMD stiffness	k_d	0.0442 N/m

5.5 Response due to Harmonic Support Motion

Consider the control mass is being perturbed with a harmonic force with a frequency of Ω radians per second and an amplitude of $\hat{p}$ for both the inner story damping model and the TMD model. The response can be calculated using SDOF response equation shown in Table 1b). The response of the TMD system can be found using the MDOF response equation shown in Table 2a). The power dissipated over the resistance can be found by differentiating the displacement response and using the time varying result (the velocity, $\dot{u}$) in the energy relationship shown in Equation (9).

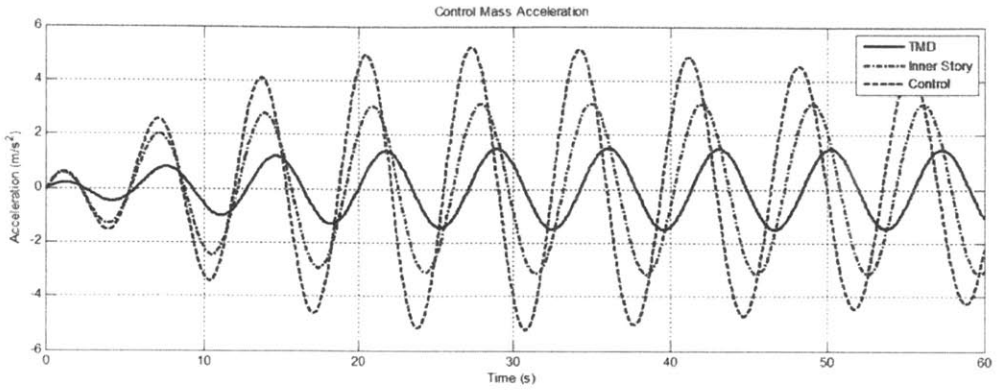

Figure 7. Acceleration response of the model at a driving frequency of 0.9 radians per second for 60 seconds of run time.

From a motion based standpoint, adding a tuned mass damper to the control toy is the best option. At a driving frequency of 0.9 radians per second, the maximum acceleration felt by the control toy, the toy with an EM damper added in parallel with the primary damper, and the EM damper acting as a TMD is 5.24, 3.17, and 1.51 meters per second squared respectively (see Figure 7).

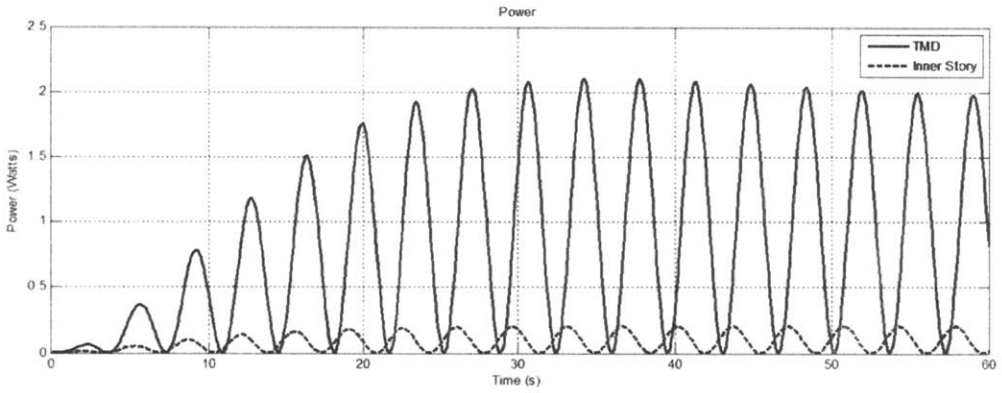

Figure 8. Power dissipated over the load resistor of the EM damper at a driving frequency of 0.9 radians per second for 60 seconds of run time.

The TMD toy also produces the most energy across the load resistor at a driving frequency of 0.9 radians per second as shown in Figure 8. In fact, for all tuning ratios, the TMD out performs the inner story damping toy in dissipating power across the load resistor as shown in Figure 9. This is because the mass for a TMD is allowed to move more than what is typically allowed for inner-story movment. Also, keep in mind that one of the same exact damper is used for both damping

strategies. Therefore, from an energy harvesting standpoint, the TMD is the more efficient of the two damping strategies.

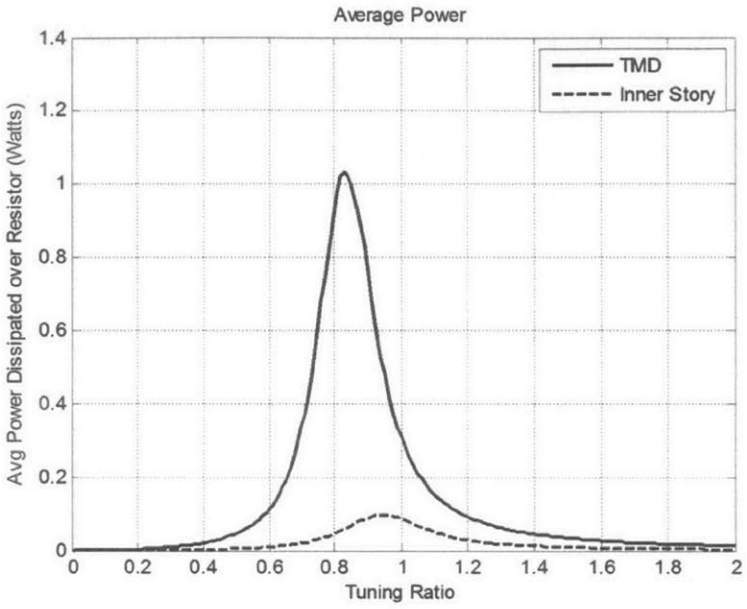

Figure 9. Average power dissipated over the load resistor for various tuning ratios.

6 Electromagnetic Damper Model

The damper used for the design application in Section 7 was adapted from the studies of Palomera-Arias (2005). The damper is a passive moving (permanent) magnet linear damper. This will be the damper used in the motion based design of a sample building in Section 7. This section will describe the similarities between the theoretical damper in Section 3 and Palomera-Arias (2005) damper, cover the main differences between the two, and develop a sample electromagnetic damper used for the design in Section 7.

6.1 Damper

Permanent magnet linear dampers are typically cylindrical in shape and typically contain a coil, a permanent magnet, iron, and a mover that creates the change in magnetic flux. There are three main configurations for a permanent magnet linear damper: 1) the mover contains the coil and moves through a cylinder composed of the permanent magnet, 2) the mover contains the iron and the magnets and coils are contained in the cylinder, and 3) the mover contains the magnet and the cylinder contains the coils. The moving magnetic option is the most suitable for electromagnetic damping because no electrical connection to the mover is required (Palomera-Arias, 2005). A cross section of the prototypical damper is shown in Figure 10. The moving magnet can be divided into poles separated by pole shoes. The machine constant is proportional to the number of poles as shown in the relationships in Equations (31).

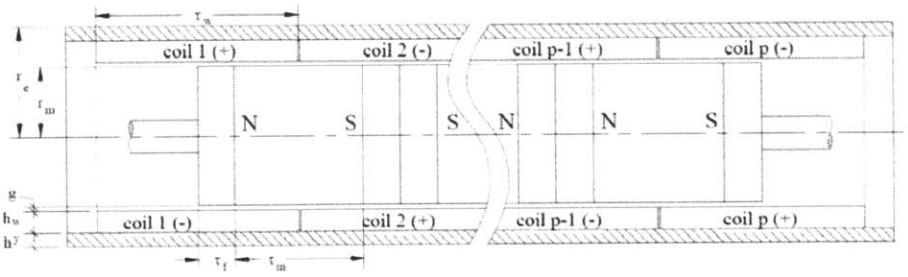

Figure 10. Tubular electromagnetic damper with p poles (Palomera-Arias, 2005).

The magnetic force for Palomera-Arias' (2005) electromagnetic damper can be derived similarly to the electromagnetic damper in Section 3. As shown in Figure 11, the circuit differs from Section 3 because the machine constant, K_t, has different parameters (the parameters are described in

Appendix A). Notice that the machine constant is proportional to the magnetic field and a length value (r_m^2/τ_w) similar to that of the theoretical damper's machine constant described in Section 3.1.

$$K_t = \frac{N_p \pi B_m r_m^2 N_w}{\tau_w} \tag{31}$$

The circuit also differs from the model in Section 3 because the electromagnetic damper has an inherent resistance, R_{coil}, and an inherent inductance, L_{coil}. The circuit is shown in Figure 11.

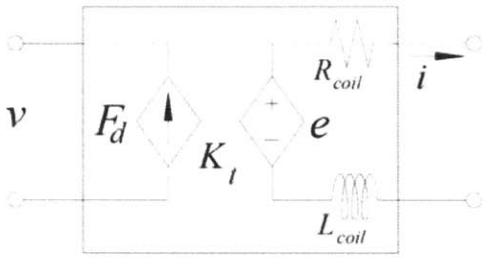

Figure 11. Electromagnetic damper circuit (Palomera-Arias, 2005).

Therefore, the equilibrium for electric potential is as follows:

$$\varepsilon - IR - L\frac{dI}{dt} = 0 \tag{32}$$

Where $R = R_{coil} + R_{load}$. Equation (32) can be modified using the relationships in shown in Equation (4).

$$K_t^2 \dot{u} - F_B R - L\frac{dF_B}{dt} = 0 \tag{33}$$

Consider the circuit under harmonic motion, $\dot{u}(t) = \hat{u}e^{i(\Omega t - \varphi)}$. The magnetic force with respect to time in the circuit can be derived from Equation (33), where c_1 depends on the initial conditions of the system.

$$F(t) = c_1 e^{-\frac{R}{L}t} + \frac{K_t^2}{R + i\Omega L}\hat{u}e^{i(\Omega t - \varphi)} \tag{34}$$

If the transient term is neglected and the absolute value of the non-transient term is taken, the magnetic force can be related to velocity.

$$F(t) = \frac{K_t^2}{\sqrt{R^2 + (\Omega L)^2}}\dot{u}(t) \tag{35}$$

6.2 Equivalent Damping

Because the magnetic force is proportional to velocity (Equation (35)), a damping coefficient can be determined. The equivalent damping coefficient of the electromagnetic damper is as follows.

$$c_d = \frac{K_t^2}{\sqrt{R^2 + (\Omega L)^2}} \tag{36}$$

There is a phase shift in the relationship of the velocity and the force due to the inductance of the coil in the damper (Palomera-Arias, 2005). The plot of Equation (35), the force-velocity relationship, is shown in Figure 12. The slope of the plot represents the damping coefficient, c_{eq}. Note that in Figure 12, as resistance increases, the elliptical shape trends towards the no delay damping line because $R^2 \gg (\Omega L)^2$ and that the damping coefficient (the slope of the plot) decreases. Both of these properties are consistent with Equation (35).

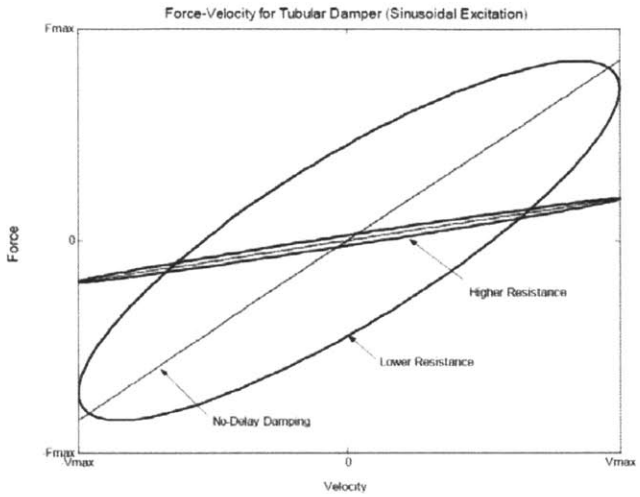

Figure 12. Force-velocity relationship with a varying resistance and a fixed inductance (Palomera-Arias, 2005).

For the damper used in the TMD model in Section 7 will have $R^2 \gg (\Omega L)^2$ and therefore the equivalent damping ratio can be approximated as:

$$c_d = \frac{K_t^2}{R} \tag{37}$$

Notice that this is an equivalent damping similar to the form as Equation (7) derived in Section 3. As seen in Equations (31) and (36), the equivalent damping coefficient, c_d, is proportional to the number of poles, N_p , in the EM damper. For convenience, values normalized by the number of poles can be obtained from Equations (31) and (36). The description and values of the parameters that make up the machine constant are detailed in Appendix A.

Table 6. Important damper machine parameters.

Machine stroke	$l_m = \tau_m$	90 mm
Machine constant (per pole)	$\frac{K_t}{N_p}$	22.017

6.3 Energy Dissipated

The current with respect to time can be equated using the relationships presented in Equation (4).

$$I(t) = \frac{K_t}{R}\dot{u}(t) \tag{38}$$

The total power dissipated by the circuit is

$$P_{tot} = P_{load} + P_{coil} = I^2 R_{load} + \left[I\left(L_{coil}\frac{dI}{dt}\right) + I^2 R_{coil}\right] \tag{39}$$

Where the power dissipated over the external load is

$$P_{load} = \left(\frac{K_t \dot{u}(t)}{R_{load} + R_{coil}}\right)^2 R_{load} \tag{40}$$

Palomera-Arias (2005) developes a relationship between the normalized power dissipated by the damper and the external load resistance using the relationships in Equations (39) and (40). The maximum power dissipated by the EM damper occurs at when $R_{load} \approx R_{coil}$. The model in Section 7 will have external load resistance equal to the coil resistance.

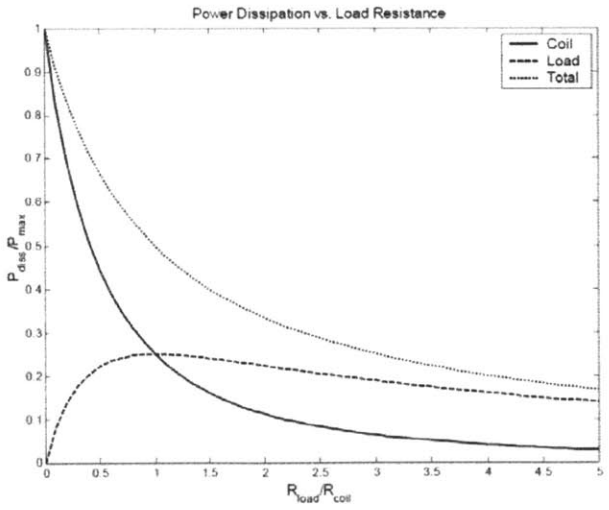

Figure 13. Damper power dissipation vs load resistance (Palomera-Arias, 2005).

Finally, the energy created by the system is simply the integral of the power with respect to time (see Equation (9)).

6.4 Damper Cost

The cost of the sample EM damper described in Table 6 is shown.

Table 7. Damper cost per pole.

Approximate damper cost (per pole)	$\frac{\$}{N_p}$	$2136.00
Approximate damper cost (per damping)	$\frac{\$}{c_d}$	$46.43 per N-s/m

This cost estimate is based on a damper with the same magnet length and radius as a sample damper machine cost in Palomera-Arias' (2005) study. The cost estimate is based on the cost of the damper material solely, not cost the installation, stiffeners or the damping mass. A reason for such a high cost per damping (a viscous damper with a similar stroke costs $2.54 per kN-s/m) is that permanent magnet composition and manufacturing processes are under patent and are currently very expensive materials (Palomera-Arias, 2005) .

7 Motion Based Design Model with an EM Damper

Motion based design, or performance based design, is the design of a structure for dynamic loading according to serviceability constraints. These serviceability constraints require that the response of the structure due to dynamic loading must not exceed a certain design acceleration (humans can start to feel movement at an acceleration of 2% of the gravitational acceleration) or story drift (displacement). Motion based design has become more prominent recently because of the following (Connor, 2003):

1. Buildings have started to become more flexible (i.e. taller) and therefore have a much greater magnitude of response due to dynamic loading,
2. Laboratories and motion sensitive manufacturing plants require the mitigation of outside movement in order to precisely calibrate and produce instruments and products, and
3. Although there has been increase in the technology of strength of materials, the stiffness (or the lack of flexibility) of these materials have remained constant.

This section will go through the motion based design of a sample six-story building under wind and earthquake loading using a tuned mass electromagnetic damper. The purpose of this section is to go through the TMD design process and to determine if using an electromagnetic damper to harvest energy is feasible.

7.1 Control Building

The control building will be a six-story building with 3m floor heights and a 12mx12m square base. Lateral load is resisted by a steel moment frame. Each bay is 6m long and the slab on each floor is 9cm thick reinforced concrete (a density of 2400 kg per cubed meter). The typical column is a W27x193 and the typical girder is W27x102. The inherent damping of the control building frame will be assumed to be 2%.

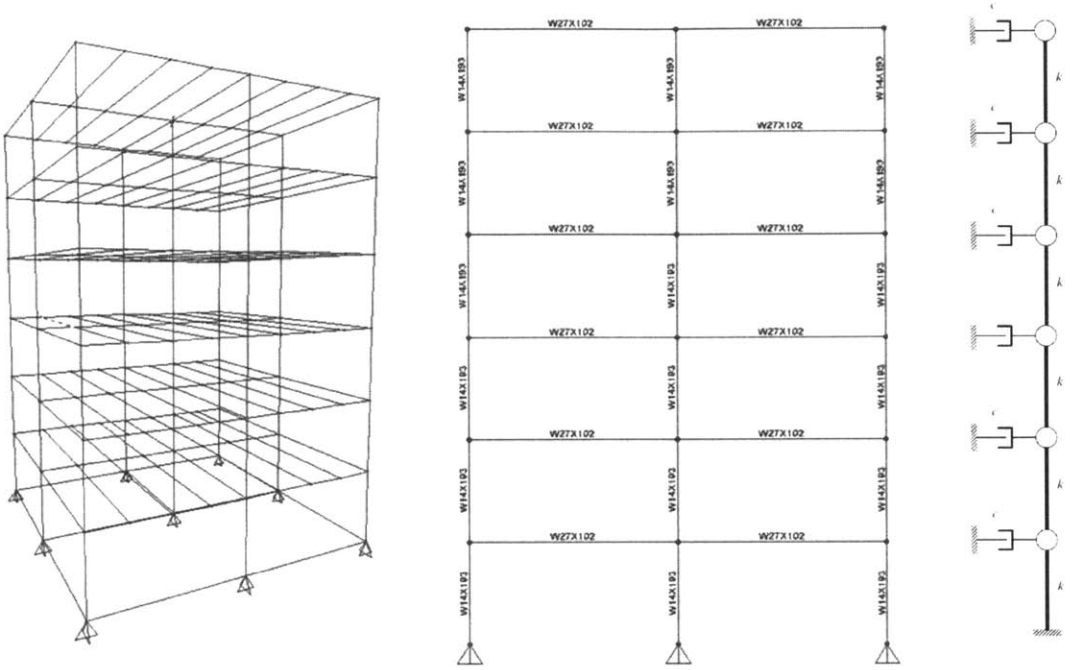

Figure 14. Left: 3D control building; Center: frame consists of three of these identical frames; Right: simplified lumped mass model.

For simplification, the 3D building will be modeled as a lumped mass model. The lumped mass model will represent the entire 3D structure (instead of representing each 2D frame) because there will be one damper placed in the center of the top floor. Therefore the total mass, m, of each floor represents the mass at each node, the stiffness of each floor, k, will include all of the stiffnesses of the columns with respect to their weak axis of each frame of a particular floor. The 3D frame, a 2D frame with member sizes, and the 1D lumped mass model are shown in Figure 14. The lateral load is considered acting on the side of the building so that each column is considered acting in its weak axis. Taking into account the stiffnessses of the columns, the mass of the floors, and the primary damping of the steel frame (estimated at 2%), the natural period of the undamped control building can be calculated to be 0.3524 seconds using strategies described in detail in Section 4.2. The detailed calculations (done in MATLAB) can be seen in Appendix B.

Table 8. Lumped mass model parameters (each floor has these values).

Floor mass	m	31,104 kg
Floor stiffness	k	170,110 kN/m
Floor damping	c	92.010 kN-s/m

The **M**, **K**, and **C** matrices can be created using a similar method to the matrices in Section 5.4.

7.2 Electromagnetic Tuned Mass Damper

The results in Section 5 show that the strategy that yields the most harvested energy is the tuned mass damper. Therefore, that strategy will be used in this experiment. The Palomera-Arias (2005) example damper as described in Section 6 will be tuned accordingly and attached to the control building's roof center and will damp purely in the direction of the columns' deflection (in their weak axis) due to lateral loading. The design constraint of the building is that the TMD displacement must not exceed the machine stroke of 90 mm. A mass ratio, $\bar{m}$, of 8% of the effective modal mass of the first mode, $\tilde{m}_{1e} = \tilde{m}_1/\phi_{16}$, will keep the damper mass from displacing more than 90 mm for both the wind and earthquake loading described in the next section, where ϕ_{16} is the mode shape value at the top floor due to the first mode. The optimal damping ratio can then be determined by Equation (41) (Tsai & Lin, 1993):

$$\xi_{d,opt} = \sqrt{\frac{3\bar{m}}{8(1+\bar{m})(1-0.5\bar{m})} + (0.151\xi_1 - 0.170\xi_1^2) + (0.163\xi_1 + 4.980\xi_1^2)\bar{m}} \tag{41}$$

The optimal frequency ratio can also be determined (Tsai & Lin, 1993):

$$f_{d,opt} = \left(\frac{\sqrt{1-0.5\bar{m}}}{1+\bar{m}} + \sqrt{1-2\xi_1^2} - 1\right) - \left(2.375 - 1.034\sqrt{\bar{m}} - 0.426\bar{m}\right)\xi_1\sqrt{\bar{m}} - \left(3.730 - 16.903\sqrt{\bar{m}} - 20.496\bar{m}\right)\xi_1^2\sqrt{\bar{m}} \tag{42}$$

Where ξ_1 is the modal damping ratio for mode 1. Therefore the optimal stiffness needed to achieve this ratio for the damper is:

$$k_d = \bar{m} f_{opt}^2 k \tag{43}$$

The optimal values for the model are shown in Table 9.

Table 9. Optimal values for the TMD.

TMD mass	m_d	2,359 kg
TMD damping ratio	$\xi_{d,opt}$	0.1709
TMD damping coef	c_d	45.23 kN-s/m
TMD stiffness	k_d	4,105 kN/m

Now that the damping and stiffness parameters have been optimized for the building, the number of poles required for the EM damper can be determined using c_d from Table 9 and c_d/N_p from Table 6.

$$N_p = \frac{c_d}{(c_d/N_p)} \tag{44}$$

To tune the damper for this particular control building, the number of poles required is 982. This is a large number of poles for one damper, so multiple dampers will most likely have to be used to create 45.2 kN-m/s damping. The cost of this amount of damping using the sample EM damper will therefore be approximately $2.1 million using the relationship in Table 6.

7.3 Loading Data

7.3.1 Wind Data

In order to accurately model the effects of wind loading on the building, wind data must be recorded at a much higher frequency than the frequency of the control building ($f_n = 2.84$Hz). Wind velocity recorded at a frequency of 5 Hz near the San Gorgonio wind farm in southern California was graciously provided by Kurt Hansen and Gunner Larsen (1991). This particular data was recorded from 12:15 to 1:15PM on March 11, 1991 from an anemometer 20m above the Earth's surface. More specifics on the data can be seen in Table 10.

Table 10. Wind data site information (Hansen & Larsen, 1991).

Site	Gorgonio
Site Classification	Hill (rolling hills), scrub (bushes and small trees)
Country	US
Position	33°56'52"N 29°W'116"36
Surface altitude	539 m
Date recorded	March 11, 1991
Average speed	23.6 m/s

The site of the wind data has a much higher average speed than the average wind speed of a typical city and therefore the magnitudes of speed in the unmodified data are not useful for this example. However, the changes in amplitude of the wind speed over time can be used to model a time varying load on the control building. In order to make the data relevant to wind force felt by an office building in a typical city (Boston), the following modifications have been made to the data:

1. The wind speed of the data has been multiplied by a factor so that the average wind speed of the data equals 5.5 m/s, the average yearly wind speed of Boston (National Climatic Data Center).
2. The assumption that the average wind speed is recorded at the base of the control building. The wind profile with respect to height was taken from the Table 6-3 in ASCE 7 and a factor, K , was determined at each of the six floor heights, where $K = 1.00$ at the base of the building (see Figure 15).

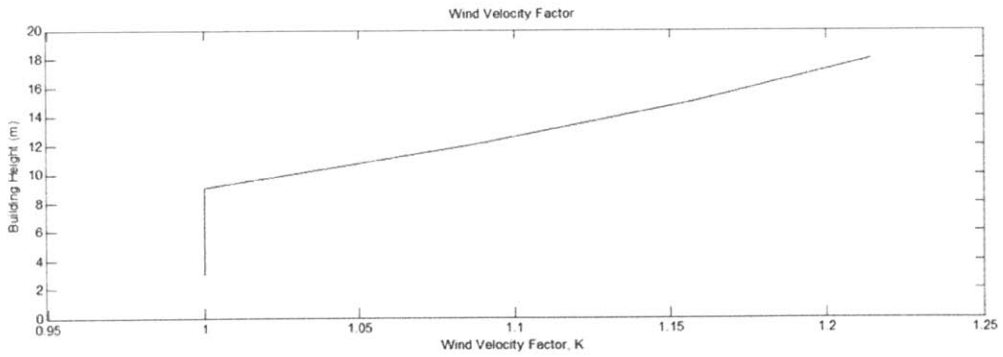

Figure 15. Wind velocity factor wrt building height.

3. The force of the wind on node n with respect to time can then calculated using Equation (45):

$$p_n(t) = \frac{1}{2} K A_t \rho_a v_w^2 \tag{45}$$

Where $A_t = 18\ \mathrm{m}^2$ is the tributary area perpendicular to the wind of each node of the control building, $\rho_a = 1.25\ \mathrm{kg/m}^3$ is the density of air, and $v_w(t)$ is the velocity of the wind with respect to time. The figure below shows a 30 second (out of 3,600 seconds) sample of the adjusted wind velocity data to show the precision and the variability of the data.

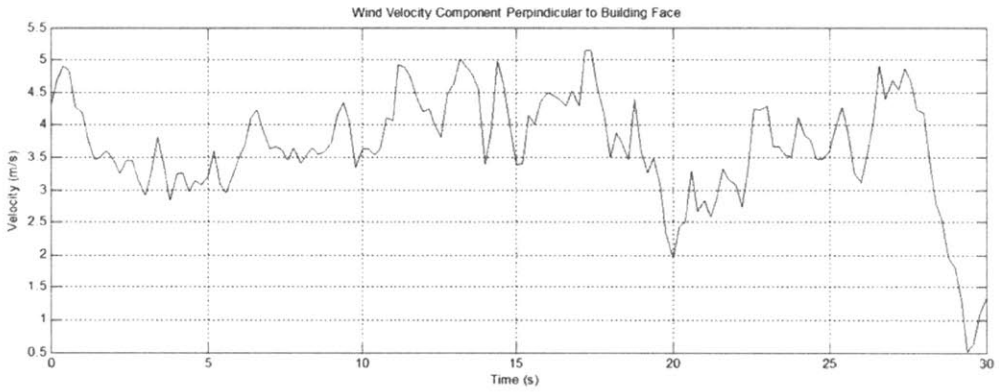

Figure 16. Thirty second sample of the adjusted wind velocity data. The velocity is the component of the velocity in the direction perpendicular to the face of the building.

The modified data, in terms of $p_n(t)$, can then be used to create the **P** matrix and the modal loading from the first mode, $\tilde{p}_1$.

$$\mathbf{P} = \begin{bmatrix} p_1(t) \\ p_2(t) \\ p_3(t) \\ p_4(t) \\ p_5(t) \\ p_6(t) \end{bmatrix} \qquad \tilde{p}_1 = \boldsymbol{\phi}_1^{\mathrm{T}} \mathbf{P}$$

7.3.2 Earthquake Data

The El Centro earthquake was also applied to the control and damped building. The ground acceleration data was retrieved at vibrationdata.com. The data was recorded at a resolution of 50 Hz and the earthquake lasted approximately 53.74 seconds. Using the data, the modal force with respect to time can be determined:

$$\tilde{p}_1 = -\Gamma \tilde{m} \ddot{u}_g$$

Where $\Gamma = \phi_{16} m \sum_n \phi_{1n} / \widetilde{m_1}$.

7.4 Results

7.4.1 Wind

The motion of the building for both the control and the TMD case can be solved using strategies described in Section 4.2. As seen in sample 30 second plot of the top node acceleration in Figure 17, the acceleration magnitude of the top floor has been greatly reduced with the TMD. The top node of the control building experienced a maximum acceleration magnitude of 0.34% of gravitational acceleration (g) while the TMD top floor experienced a maximum acceleration magnitude of 0.14% g.

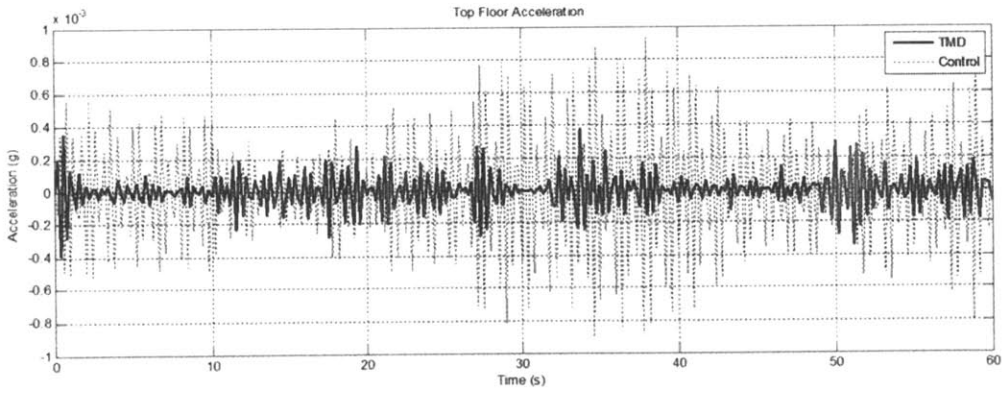

Figure 17. Dynamic results of the building under sample wind loading for the first 60 seconds

The energy harvested due to the hour long wind loading sample is the area under the plot of Figure 18, which is 3,091 Watt-hours. The average power, $P_{avg} = W/t$, for the one hour interval is 51.52 Watts. If this is considered as the average energy harvested in an hour for the average day, the total

energy harvested per year would be 27,078 kWh. Taking the price of a kWh in Boston as approximately $0.15, the total cost saved by the system is $4,062 per year.

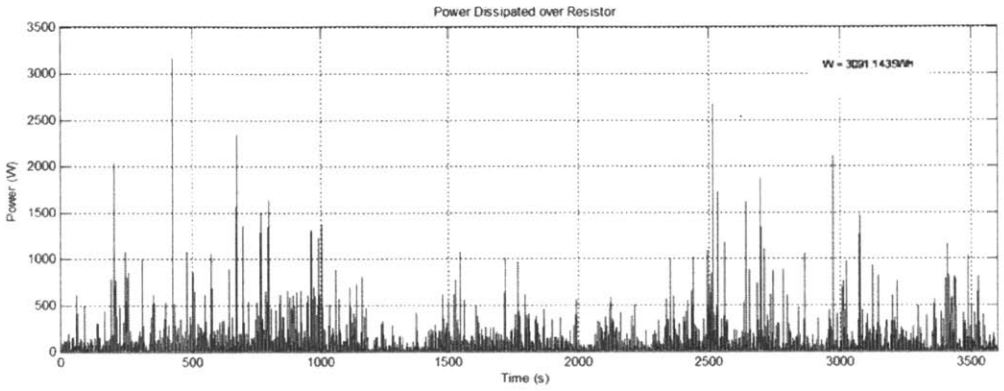

Figure 18. Power dissipated over the loading resistor with respect to time due to the one hour sample wind loading.

7.4.2 Earthquake

The motion of the building for both the control and the TMD case can be solved using strategies described in Section 4.2. As seen in the 60 second plot in Figure 19, the acceleration magnitude of the top floor has been greatly reduced with the TMD. The maximum acceleration that the control building experiences is 137% of g, while adding the TMD will reduce the maximum acceleration to 49% g.

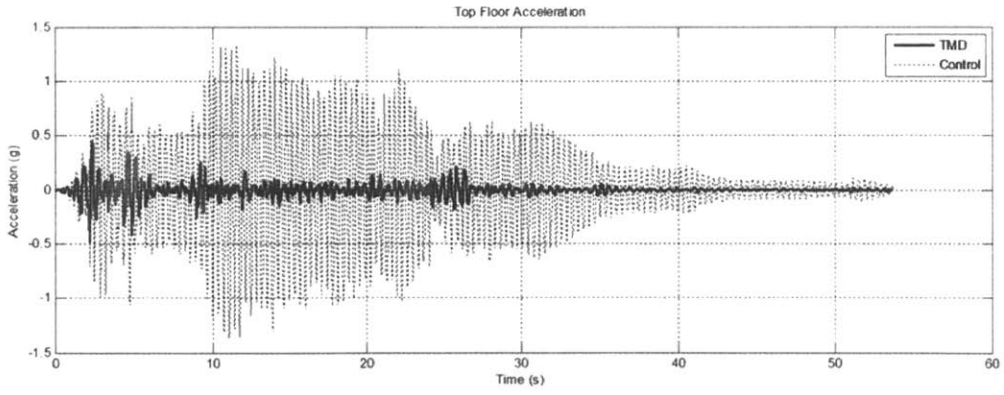

Figure 19. The acceleration of the top floor of the TMD building and the control building due to the El Centro earthquake.

The energy harvested due to the 54 second long earthquake is 35.5 kWh, resulting in a savings of $5.33 worth of energy. The average power, since the earthquake happens at a much smaller time scale and with larger forces, is much higher than that of the wind loading, at 2.378 MW.

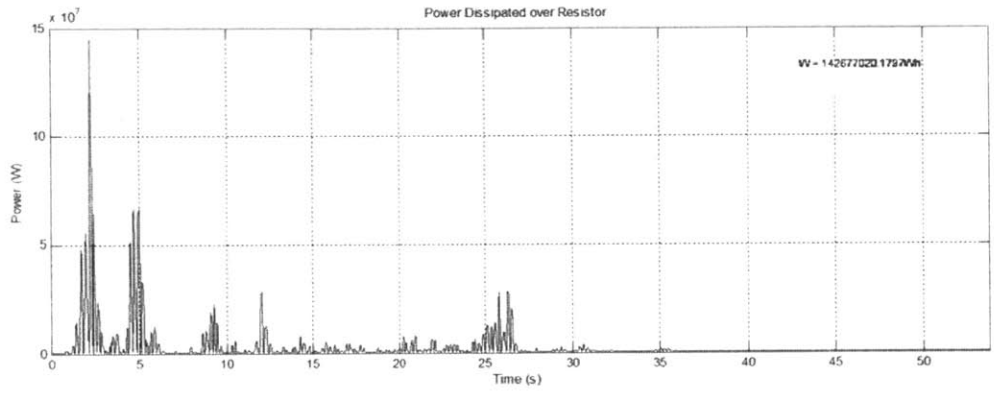

Figure 20. Power dissipated over the loading resistor with respect to time due to the 54 second El Centro earthquake loading on the TMD building.

7.5 Summary

7.5.1 Wind Loading Results Summary

The building is slightly stiff compared to the period approximation method of the number of floors divided by ten. The approximated period is 0.6 seconds while the actual period is 0.35 seconds. A stiffer building reduces movement. Therefore, the wind acting on the building has a negligible effect with regards to human perception of movement (humans can feel 2% g or higher). The maximum acceleration of the building was reduced by 50% to 0.01% g, which may be helpful for labs or machine equipment with high precision capabilities. This small sustained movement reduction generated an average power of 51.52 Watts over the resistor in the EM Damper system. This average power sustained over a full year will produce over $4,000 of energy savings.

Table 11. Wind loading results table.

Variable	Control Building	Building w/ TMD
Natural period	0.352 s	0.429 s
Damper cost	0	$2.1 million
Maximum top floor acceleration	0.0034g	0.0014g
Average power generated over resitor	0	51.52 W
Estimated energy cost savings per year	0	$4,062 per year

7.5.2 Earthquake Loading Results Summary

An earthquake like El Centro happens very rarely, so the generated power from the earthquake is almost negligible in determining if the EM damper system is feasible. However, it is interesting to see how much electric energy can be harvested in an earthquake. From a motion based design perspective, the TMD adequately reduced the acceleration of the top floor from 1.37g to 0.49g. Since the earthquake has such a short duration (less than 60 seconds) the total amount of energy harvested from the perturbation is only worth $5.33.

Table 12. Earthquake loading results table.

Variable	Control Building	Building w/ TMD
Natural period	0.352 s	0.429 s
Damper cost	0	$2.1 million
Maximum top floor acceleration	1.37 g	0.49 g
Average power generated over resistor	0	2.378 MW
Estimated energy cost savings per earthquake	0	$5.33 per earthquake

8 Conclusion

The purpose behind this research was to determine the feasibility of harvesting electricity via electromagnetic damping for larger scale structures. The research has shown that passive electromagnetic dampers can harvest energy by dissipating kinetic energy.

The model toys in Section 5 show that motion control and energy harvesting is best utilized using a tuned mass damper design. The model shows that if another mass is attached to a tuned EM damper, the model produces on the order of 10 times more energy across the resistor at a tuning ratio of 0.9 than if the same damper was connected in parallel with the spring and primary damper of the model. The model also shows that the acceleration amplitude with the TMD EM damper is less than the amplitude of the inner story EM damper when both primary masses are under the same harmonic loading.

The most efficient damper for large scale applications is the moving magnet tubular, linear damper, as described in Section 6. A linear damping coefficient can be determined for the damper if the inductance is much less than the resistance of the system. The power dissipated over the load resistor is maximized when the resistance of the coil equals the resistance of the load connector. The economic cost of the damper, however, is far more (on the order of 1,000 to 10,000 times more) than a retail viscous damper with the same damping coefficient.

The six-story structure with a passive EM TMD in Section 8 shows that a small amount of energy is created via the damping of the building under sample wind loading (an average power of around 51 Watts). Since the amount of energy harvested by the EM damper depends on the amount of movement of the mover, and because large scale structures are typically designed to prevent movement, the small scale movements aren't enough to create enough energy to outweigh the cost of the EM damper. The current cost of the damper is on the order of 1,000 times more than the yearly benefit of power savings making a breakeven point of the damper system unreachable if just considering the economic benefits of the energy saved. Therefore, it can be concluded that due to the small scale movements of large structures and the cost of dampers for large scale forces, energy harvesting, passive EM dampers are currently not economically feasible for large scale structures.

Bibliography

Connor, J. (2003). *Introduction to Structural Motion Control.* Upper Saddle River, NJ: Pearson Education.

Ebrahimi, B., E., Khamesee, M., & Gonarachi, F. (2009). Eddy current damper feasibility in automobile suspension: modleing, simulation and testing. *Smart Materials and Structures*, 1-12.

El Centro Earthquake Page. (1940, May 18). Retrieved April 29, 2013, from Vibration Data: http://www.vibrationdata.com/elcentro.htm

Hansen, K., & Larsen, G. (1991, March 11). *Database of Wind Characteristics.* Retrieved April 25, 2013, from Wind Data: http://www.winddata.com/

Kausel, E. (2009). Advanced Structural Dynamics (Course Notes).

Palomera-Arias, R. (2005). *Passive Electromagnetic Damping Device for Motion Control of Building Structures.* Cambridge, MA: Massachusetts Institute of Technology.

Tang, X., & Zuo, L. (2012). Simultaneous energy harvesting and vibration control of structures with tuned mass dampers. *Inteligent Material Systems and Structures*, 2117-2127.

Tsai, K., & Lin, G. (1993). Optimum Tuned-Mass Dampers for Minimizing Steady-State Response of Support-Excited and Damped Systems. *Earthquake Engineering and Structural Dynamics*, 957-973.

Zuo, L., & Zhang, P. (2013). Energy harvesting, ride comfor, and road handling of regenerative vehicle suspensions. *Journal of Vibration and Acoustics* , 1-8.

Appendix A. Model Damper Parameters

$$K_t = \frac{N_p \pi B_m r_m^2 N_w}{\tau_w} \tag{46}$$

The sample tuned mass damper in Section 7 will have the following parameters:

Table 13. Tuned EM damper, adjusted from Palomera-Arias (2005)

Magnet length	τ_m	90 mm
Pole shoe width	τ_f	15.1 mm
Coil length	$\tau_w = \tau_m + 2\tau_f$	120.2 mm
Magnetic field	B_m	1.2 T
Mover radius	r_m	60 mm
Coil turns	N_w	195
Load resistance	R_{load}	10.3 Ω
Coil resistance	R_{coil}	10.3 Ω
Coil inductance	L_{coil}	5.1 mH

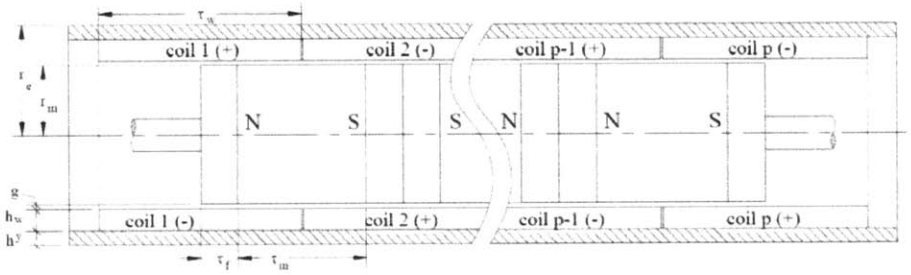

Appendix B. Model MATLAB Code

```
%************************************************************************
%MODEL PARAMETERS*******************************************************
%************************************************************************

figs =true; %true = on
analysis = 0; %0=earthquake, 1=wind

%BUILDING DIMENSIONS
dof = 6;                        % num of floors
g = 9.80665;                    % m/s^2
h = 3;                          % floor height, m
H = [3;6;9;12;15;18];           % floor elevations, m
Lb = 6;                         % bay length, m
nBays = 2;                      % number of bays
Atw = nBays*Lb*h;               % trib area perp. to wind
Afloor = (2*Lb)*(2*Lb);         % floor area
tfa = 300;                      % kWh per m^2 floor area per year

%Energy
energyCost = 0.15;              % cost per kWh
Wcons = dof*Afloor*tfa;         % kWh per year of building

if analysis==0
    %EARTHQUAKE DATA
    ddug = load('quake');       % reads the quake file and stores it in the
vector "accg"
    ddug = ddug/1000;           % convert quake acceleration from mm/s^2 to m/s^2
    dt = 0.02;                  % time step of earthquake
    n = length(ddug);           % number of points in earthquake
    td = (n-1)*dt;              % duration of earthquake
    t = 0:dt:td;                % time vectort)
else
    %WIND DATA
    t = struct2array(load('wdTime'))'; % reads wind data time values
    dt = 1/5;                   % wind data time step, s
    n = length(t);              % num data points
    avgSpeed = 12.4;            % avg wind speed Boston, mph
    avgSpeed = avgSpeed*0.44704;% avg wind speed, m/s
    windProf = [.7; .7; .7; .76; .81; .85]; % wind profile
    windProf = windProf/min(windProf); % normalized wind profile
    vWind = struct2array(load('wd1235'))';% wind velocity data, m/s
    vAvg = mean(vWind);         % average wind speed of data
    vWind = vWind*(avgSpeed/vAvg); % reduced wind speed
    rhoAir = 1.25;              % density of air, kg/m^3
    Pw = zeros(dof,n);          % wind force, N
    for i=1:dof
        if(i==dof)
            Pw(i,:) = 1/2*rhoAir.*vWind.^2*windProf(i)*Atw;
        else
            Pw(i,:) = 1/2*rhoAir.*vWind.^2*windProf(i)*(.5*Atw);
        end
    end
```

```
end


%MASS
rhoc = 2400;                % concrete density, kg/m^3
tslab = .09;                % slab thickness, m
m = tslab*Afloor*rhoc;      % floor mass, kg

%STIFFNESS
E = 200e9;                  % steel modulus, N/m^2;
Ic = 931;                   % column moment, W27x193, weak axis, in^4
Ic = Ic*4.16231426e-7;      % column moment, m^4
Ib = 3620;                  % beam moment, W27x102, strong axis, in^4
Ib = Ib*4.16231426e-7;      % beam moment, m^4
r = Ic*Lb/h/Ib;
kint = 12*E*Ic/(h^3*(1+r)); % interior column stiffness, N/m
kext = 12*E*Ic/(h^3*(1+2*r));% exterior column stiffness, N/m
k = 3*(2*kext+kint);        % total floor stiffness, N/m


%PRIMARY DAMPING
xi = 0.02;                  % primary damping ratio
c = 2*xi*sqrt(k*m);         % primary damping coeff, N-s/m

%EM DAMPER
Rload = 10.3;                 % resistance of energy harvesting decive, Ohms
poles = 1;                  % number of poles
Bm = 1.2;                   % magnetic field, T
rm = 60e-3;                 % mover radius, m
Tm = 90e-3;                 % magnet length, m
Tf = 15.1e-3;               % pole shoe width, m
Tw = Tm + 2*Tf;             % coil length, m
Nw = 195;                   % turns per coil
Kt1p = poles*pi*Bm*rm^2*Nw/Tw;% EM maching constant (1 pole), N/A
Rcoil = Rload;              % EM resistance, ohms
Lcoil = 5.1e-3;             % EM inductance, H
R = Rcoil + Rload;          % circuit resistance
cd1p = Kt1p^2/R;            % damping coeff of EM damper (1 pole), N-s/m
cost1p = 2136;


%************************************************************************
%CONTROL BUILDING*********************************************************
%************************************************************************
alpha = c/k;
M = zeros(dof);             % mass matrix
K = zeros(dof);             % stiffness matrix

for i=1:dof
    for j=1:dof
        if i==j
            M(i,j) = m;
            if i==dof
                K(i,j) = k;
            else
```

```
                K(i,j) = k+k;
            end
        else if abs(i-j)==1
                K(i,j) = -k;
            end
        end
    end
end

C = alpha.*K;                % damping matrix


%MODE SHAPE
[PHI,w2] = eig(K,M);
W = sqrt(diag(w2));          % natural frequencies
for i=1:dof
    PHI(i)=PHI(i)/PHI(dof); % mode shape
end

phi1 = PHI(:,1);             % mode 1 shape
wn1 = W(1,1);                % mode 1 nat freq, rad/sec
fn1 = wn1/(2*pi);            % mode 1 nat freq, Hz
Tn1 = 1/fn1;                 % mode 1 period, s


mm1 = phi1'*M*phi1;          % modal 1 mass
km1 = phi1'*K*phi1;          % modal 1 stiffness
cm1 = phi1'*C*phi1;          % modal 1 damping
xim1 = cm1/(2*wn1*mm1);      % modal 1 damp ratio
wnd1 = wn1*sqrt(1-xim1);     % damped nat freq, rad/s

mm1e = mm1/phi1(dof,1)^2;    % effective modal mass
km1e = km1/phi1(dof,1)^2;    % effective modal stiffness
cm1e = cm1/phi1(dof,1)^2;    % effective modal damping

%OPTIMAL DAMPING
mbar = .08;                  % mass ratio
fopt = (sqrt(1-.5*mbar)/(1+mbar)+sqrt(1-2*xim1^2)-1) - (2.375-
1.034*sqrt(mbar)-.426*mbar)*xim1*sqrt(mbar) - (3.730-
16.903*sqrt(mbar)+20.496*mbar)*xim1^2*sqrt(mbar);
xidopt = sqrt(3*mbar/(8*(1+mbar)*(1-.5*mbar)))+(.151*xim1-.170*xim1^2) +
(.163*xim1+4.980*xim1^2)*mbar;
wd = fopt*wn1;
md = mbar*mm1e;              % damper mass
kd = mbar*fopt^2*km1;                % damper stiffness
cd = 2*xidopt*wd*md;



%FORCE MATRIX
if analysis==0
    gam1 = phi1(dof,1)/mm1*m*sum(phi1);
    gam1e = phi1(dof,1)/mm1e*m*sum(phi1);
    p = mm1*gam1*ddug;
else
```

```
    pm1 = phi1'*Pw;
    pm1e = pm1/phi1(dof,1)^2;
    p = pm1;
end

%DISPLACEMENT
h = 1/(mm1*wnd1).*exp(-xim1*wn1.*t).*sin(wnd1.*t); % impulse response
Q = conv(p,h);              % convolution calc
q = dt*Q(1:n);              % q factor
V = phi1*q;                 % displacement relative to ground

%VELOCITY
dvc = zeros(1,n);           % velocity of top node, m/s
for i=2:n
    dvc(i)=(V(dof,i)-V(dof,i-1))/dt;
end

%ACCELERATIOM
ddvc = zeros(1,n);          % accelearation of top node, m/s^2
for i=2:length(dvc)
    ddvc(i)=(dvc(i)-dvc(i-1))/dt;
end



%************************************************************************
%DAMPED BUILDING*********************************************************
%************************************************************************
dofd = dof+1;
Md = zeros(dofd);
Kd = zeros(dofd);
Cd = zeros(dofd);

for i=1:dof
    for j=1:dof
        Md(i,j) = M(i,j);
        Cd(i,j) = C(i,j);
        Kd(i,j) = K(i,j);
    end
end

Md(dofd,dofd) = md;

Kd(dof,dof) = Kd(dof,dof) + kd;
Kd(dofd,dofd) = kd;
Kd(dofd,dof) = -kd;
Kd(dof,dofd) = -kd;

Cd(dof,dof) = Cd(dof,dof) + cd;
Cd(dofd,dofd) = cd;
Cd(dof,dof-1) = -cd;
Cd(dof-1,dof) = -cd;

%Mode Shape
```

```
[PHId,w2d] = eig(Kd,Md);
Wd = sqrt(diag(w2d));
for i=1:dofd
    PHId(i)=PHId(i)/PHId(dofd);
end

phi1d = PHId(:,1);
wn1d = Wd(1,1);
fn1d = wn1d/(2*pi);
Tn1d = 1/fn1d;

mm1d = phi1d'*Md*phi1d;
km1d = phi1d'*Kd*phi1d;
cm1d = phi1d'*Cd*phi1d;
xim1d = cm1d/(2*wn1d*mm1d);
wnd1d = wn1d*sqrt(1-xim1d);

if analysis==0
    gam1d = phi1d(dofd,1)/mm1d*m*sum(phi1d);
    pd = mm1d*gam1d*ddug;
else
    pm1d = phi1'*Pw;
    pd = pm1d;
end

%DISPLACEMENT
hd = 1/(mm1d*wnd1d).*exp(-xim1d*wn1d.*t).*sin(wnd1d.*t);
Qd = conv(pd,hd);
qd = dt*Qd(1:n);
Vd = phi1d*qd;

%VELOCITY
dvcd = zeros(1,n);
for i=2:n
    dvcd(i)=(Vd(dof,i)-Vd(dof,i-1))/dt;
end

%ACCELERATION
ddvcd = zeros(1,n);
for i=2:length(dvc)
    ddvcd(i)=(dvcd(i)-dvcd(i-1))/dt;
end


%DAMPER MASS VELOCITY
dvd = zeros(1,n);
for i=2:n
    dvd(i)=(Vd(dofd,i)-Vd(dofd,i-1))/dt;
end

%*************************************************************************
%POWER DISSIPATED*********************************************************
%*************************************************************************
```

```
%Emf
poles = cd/cd1p;
Kt = poles*Kt1p;
emf = -Kt.*dvd;

%Current
I = emf./R;

%Energy
dI = zeros(1,n);
for i = 2:n
    dI(i)=(I(i)-I(i-1))/dt;
end
Pr = abs(I.^2*Rload);
Wr = 0;
for i = 1:n
    Wr = Wr + Pr(i)*dt;
end
Wr = round(Wr*1000)/1000; %J,Ws

seconds = n*dt;
Pavgcon = Wcons*1000/(24*365)
Pavg = Wr/seconds
Wph = Wr/60/(seconds/3600); %Wh per hour
kWpy = Wph*24*365/1000; %kWh per year
pWsaved = kWpy/Wcons;
savedpy = energyCost*kWpy
damperCost = cost1p*poles




%************************************************************************
%FIGURES*****************************************************************
%************************************************************************
if figs==true
    if analysis == 1
        %Wind Force
        figure('Color',[1 1 1],'Position', [100 100 1200 400]);
        plot(t,vWind)
        title('Wind Velocity Component Perpindicular to Building Face')
        xlim([0 30])
        xlabel('Time (s)')
        ylabel('Velocity (m/s)')
        grid on
    end

    %Mode Shape
    mn = 1;
    figure('Color',[1 1 1],'Position', [100 100 400 800]);
    ms = plot([0;PHId(1:dof,mn)],[0;H],[0;PHI(:,mn)] , [0;H], ':');
    set(ms(1),'linewidth',3);
    set(ms(2),'linewidth',3);
    xlim([-1 1])
    title('Mode Shape')
```

```
    ylabel('Height')
    legend('TMD','Control');
    grid on

    %Top Floor Displacement
%     figure('Color',[1 1 1],'Position', [100 100 1200 400]);
%     plot(t,Vd(dof,:), t,V(dof,:), ':')
%     title('Top Floor Displacement')
%     xlim([0 60])
%     xlabel('Time (s)')
%     ylabel('Displacement (m)')
%     legend('TMD','Control');
%     grid on

    %Top Floor Acceleration
    figure('Color',[1 1 1],'Position', [100 100 1200 400]);
    tfa = plot(t,ddvcd/g, t,ddvc/g, ':')
    set(tfa(1),'linewidth',2);
    set(tfa(2),'linewidth',1);
    title('Top Floor Acceleration')
    xlim([0 60])
    xlabel('Time (s)')
    ylabel('Acceleration (g)')
    legend('TMD','Control');
    grid on

    %TMD Mass Displacement
    figure('Color',[1 1 1],'Position', [100 100 1200 400]);
    plot(t,Vd(dofd,:))
    title('TMD Mass Displacement')
    xlim([0 max(t)])
    xlabel('Time (s)')
    ylabel('Displacement (m)')
    grid on

%     %TMD Mass Velocity
%     figure('Color',[1 1 1],'Position', [100 100 1200 400]);
%     plot(t,dvd)
%     title('TMD Mass Velocity')
%     xlim([0 max(t)])
%     xlabel('Time (s)')
%     ylabel('Velocity (m/s)')
%     grid on

    %Power Dissipated
    figure('Color',[1 1 1],'Position', [100 100 1200 400]);
    plot(t,Pr)
    title('Power Dissipated over Resistor')
    xlim([0 max(t)])
    xlabel('Time (s)')
    ylabel('Power (W)')
    uicontrol('Style', 'text', 'String', strcat(['W = ',num2str(Wph), 'Wh']),
'Units','normalized','Position', [0.75 0.75 0.1 0.1]);
    grid on

end
```